Investigate the effect of hydrothermal temperature on the structure and characterization of 20 % ZnO-Cu_2O nanocomposite

Nguyen Thi Tuyet Mai, Nguyen Thi Lan, Nguyen Kim Nga, Ta Ngoc Dung, Huynh Dang Chinh

School of Chemical Engineering, Hanoi University of Science and Technology, Ha Noi, Vietnam
mai.nguyenthituyet@hust.edu.vn

Abstract

The ZnO with 20 mol.% was hybridized with Cu_2O to fabricate nanocomposites (20 % ZnO-Cu_2O (ZC NCs)) were prepared by hydrothermal method at the investigated temperatures of (120, 200 and 250) ℃. The structural properties and characterization of the materials were investigated by physical measurements including: XRD, SEM, EDX and solid sample UV-Vis spectra. The results showed that the fabricated material samples consist of two crystalline phases (ZnO wurtzite and Cu_2O octahedra) with calculated lattice parameters that were suitable for each type of crystal of the material. The average crystal sizes of the ZC120, ZC200 and ZC250 samples were (20.08, 20.36 and 22.50) nm respectively, which were grown lager when the hydrothermal temperature increase. The optical bandgap energy (Eg) of the ZC_{120}, ZC_{200} and ZC_{250} material samples was determined to be (2.51, 2.52 and 2.56) eV, respectively. These Eg values of the fabricated ZC NCs samples were intermediate between the two types of ZnO (Eg ~ 3.37 eV) and Cu_2O (Eg ~ 2.17 eV) materials, and was valid in the excitation region of visible light.

Received 18/01/2023
Accepted 10/07/2023
Published 31/07/2023

Keywords
Cuprous oxide, ZnO-Cu_2O nanocomposite, ZnO doped Cu_2O nanoparticles, visible light irradiation

1 Introduction

Nanocomposites (also known as hybrid or grafting materials) between two or more different types of semiconductors have been and are being studied. Because these materials have enhanced beneficial properties compared to single materials. For example, Cu_2O@TiO_2 composite materials, $Zn_{1-x}Cu_xO$ hybrid materials, Cu_2O-ZnO nanocomposites, Fe_2O_3 doped ZnO nanostructured materials, etc. These nanocomposites have enhanced the beneficial properties such as reducing the nanocrystal particle size, increasing the porosity of the material, and reducing the band gap energy more than semiconductors which have with the wide optical band gap energy [1-4]. These properties of materials are desirable properties to be improved in order to enhance efficiency in the field of application of the material such as: the application range uses light in the visible region, enhancing the efficiency of photogenerated electron-hole pairs separation and reducing the recombination rate of these electron-hole pairs [3-5]. The ZnO semiconductor material is one of the unique semiconductor materials with a wide direct optical band gap (Eg ≈ 3.37 eV) and a high exciton binding energy of 60 meV. ZnO is a material studied in many fields of application such as sunscreen, colorants, food additives, photocatalysts for pollution control, antibacterial agents, optical biosensors, nano-luminescent material [6,7]. The Cu_2O semiconductor material is a p-type semiconductor that is characterized by its narrow optical band gap energy Eg ≈ (2.0-2.2) eV. The diverse applications using Cu_2O are solar cells, fungicides, antibacterial agents, catalysts using

sunlight, gas sensors, biosensors [8-11]. The fabrication of composite materials (hybrid or grafting materials) between two types of ZnO and Cu_2O materials is one of the currently interested and researched composite materials systems. Composite materials between ZnO and Cu_2O achieve more beneficial properties than single materials in terms of reducing the crystal grain size; reducing the band gap energy (compared to the wide bandgap energy of ZnO); improving the separation efficiency and reducing the photogenarated electron-hole recombination rate of single materials [5,7,8,11-21]. In the content of this research, we present the investigation of the influence of different hydrothermal temperatures on the structural properties and characterizations of 20 % ZnO-Cu_2O nanocomposites (ZnO of 20 mol% doped Cu_2O materials, designated as ZC NCs).

2 Materials and methods

2.1 Used chemicals

Zinc nitrate hexahydrate ($Zn(NO_3)_2.6H_2O$ 99 %, AR-China); Copper(II) sulfate pentahydrate ($CuSO_4.5H_2O$ 99.8 %, AR-China); Sodium hydroxide (NaOH 99 %, AR-China); hydrazine hydrate ($N_2H_4.H_2O$ 80 %, AR-China); Double distilled water.

2.2 Experimental process

A solution consisting of 0.25M $Zn(NO_3)_2$ solution and 1M NaOH solution (taken according to the molar ratio of Zn^{2+}:Na^+ = 1:1.6) was stirred uniformly on a magnetic stirrer for 15 minute (solution A). Another mixed solution including 0.25M $CuSO_4$ solution, 1M NaOH solution and $N_2H_4.H_2O$ solution (with the molar ratio Cu^{2+}:Na^+:N_2H_4 = 1:1.6:0.32) also was stirred uniformly on a magnetic stirrer for 60 min at a heating temperature of 75 ℃ (solution B). Next, mixed solution A was slowly added to mixed solution B to get mixed solution C and continued to stir this mixed solution C for another 30 minutes (in which, the amount of $Zn(NO_3)_2$ mixed with $CuSO_4$ in mixed solution C according to the molar ratio of Zn^{2+}:Cu^{2+} = 0.2:1). Finally, the mixed solution C was transferred to the autoclave and hydrothermally heated at the temperatures of (120, 200 and 250) ℃ for 6 hours. The paste powder sample after hydrothermal process was washed by centrifugation several times with double distilled water until the sample reached pH ≈ 7. These clean paste powder samples was dried at 90 ℃ for 24 hours. The obtained products were light reddish brown fine powder samples that were 20 % ZnO-Cu_2O nanocomposites (ZC NCs). The sample symbols corresponding to the above hydrothermal temperatures were of ZC_{120}, ZC_{200}, ZC_{250}, respectively.
+ The methods for measuring material characterizations include: X-ray diffraction (XRD, X'pert Pro, Cu-Kα radiation λ = 1.54065 Å, scanning speed 0.03º/2s); Scanning electron microscopy (SEM, TM4000 Plus); X-ray energy scattering spectra (EDX, Oxford 300); Solid UV-Vis absorption spectra (Jasco V-750), 60 mm integrated sphere (ISV-922).

3 Results and discussion

3.1 X-ray diffraction results (XRD)

The X-ray diffraction (XRD) spectra of the ZC_{120}, ZC_{200} and ZC_{250} nanocomposites (20 % ZnO-Cu_2O nanocomposites) were shown in Fig. 1a, Fig. 1b and Fig. 1c, respectively. Fig. 1d was the superimposed XRD spectra of the ZC_{120}, ZC_{200}, ZC_{250} nanocomposite samples. The XRD spectra in Fig. 1(a,b,c,d) shows that the ZC_{120}, ZC_{200}, ZC_{250} samples all had diffraction peaks at the diffraction angle positions 2θ ≈ 42.4º and 50.9º corresponded to the (200) and (211) diffraction planes of octahedra phase Cu_2O [5,8,9,11]. Diffraction spectra of ZC_{120}, ZC_{200} samples (Fig. 1a, Fig. 1b) shows that there were more diffraction peaks at position 2θ ≈ 36.5º corresponding to the (111) diffraction plane of octahedra phase Cu_2O [5,8,11]. The ZC_{200}, ZC_{250} material samples (Fig. 1b, Fig. 1c) observed that there were diffraction peaks at the positions of diffraction angle 2θ ≈ 31.5º, 34.2º, 36.04º and 56.4º. This 2θ positions corresponds to the (100), (002), (101) and (110) diffraction planes of wurtzite phase ZnO [2,3,5]. The XRD spectrum of the sample ZC_{120} observed that there was one peak at position 2θ ≈ 36.04º corresponding to the (101) plane of the wurtzite phase ZnO [2,3,5]. In addition, on the XRD spectra of the material samples observed that the diffraction peaks were widened, and no strange diffraction peaks appeared other the diffraction peaks corresponding to the Cu_2O and ZnO crystal phases above. The higher the hydrothermal temperature of the samples (120-250) ℃, the larger and sharper the diffraction peak intensity observed.

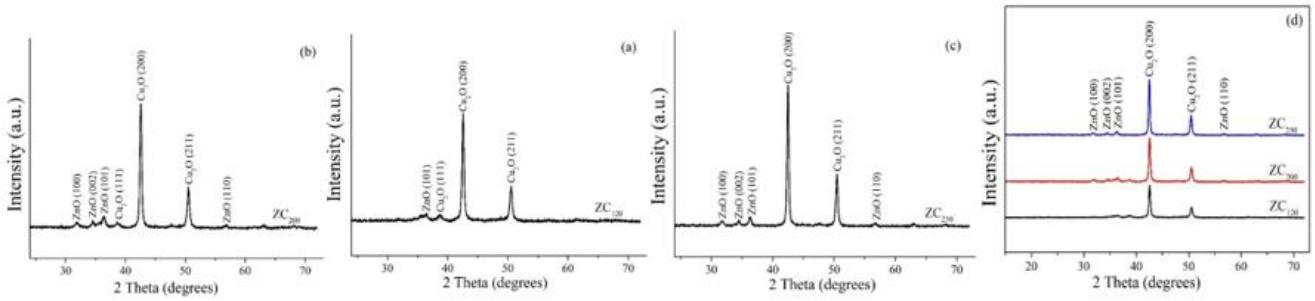

Fig. 1 (a,b,c,d). XRD spectra of ZC_{120}, ZC_{200} and ZC_{250} nanocomposite samples

This could be commented that at increasing hydrothermal temperature, the crystallinity of the material sample was better (ZC_{250} hydrothermal sample at 250 ℃). Based on observations from XRD spectra of the samples of ZC_{120}, ZC_{200} and ZC_{250} samples above, it can be determined that these fabricated material samples have been crystalline in two crystalline phases of ZnO wurtzite and Cu_2O octahedra. The intensity of the peaks corresponding to the ZnO crystalline phase was much smaller than the peak intensity of the Cu_2O crystalline phase. This could be explained because the doping of ZnO into Cu_2O was small (with a small amount of 20 mol%). Apply the Debye Scherrer equation [2,5,11] to the crystal face with the intensity of the strongest diffraction peak (at 200 plane) to determine the average crystal size of the ZC_{120}, ZC_{200} and ZC_{250} material samples. The lattice parameters of the samples were also calculated for two types of ZnO and Cu_2O crystalline phase in each material sample [5,9,11]. The results on the average crystal size and lattice parameters of the ZC_{120}, ZC_{200}, ZC_{250} samples were given in Table 1.

Table 2 The average crystal size, lattice parameters of the ZC_{120}, ZC_{200} and ZC_{250} samples

Samples		Average crystal size, D (nm)	Lattice parameters, a, b, c (Å), V (Å^3)	
ZC_{120}	ZnO	20.08	-	-
	Cu_2O		a = b = c = 4.157	71.836
ZC_{200}	ZnO	20.36	a = b = 3.241, c = 5.188	47.193
	Cu_2O		a = b = c = 4.156	71.784
ZC_{250}	ZnO	22.50	a = b = 3.249, c = 5.198	47.518
	Cu_2O		a = b = c = 4.150	71.744

From the data in Table 1, it was shown that when the hydrothermal temperature increased from (120-250) ℃, the average crystal size also grows larger (20.08-22.50 nm). The diffraction peak intensity of sample was also increased and sharper. This could be explained that when the hydrothermal temperature of the sample was increased, the small crystals were grown and agglomerated into a larger crystal mass. The lattice parameters of the material samples (according to the calculation results in Table 1) were suitable for each type of ZnO crystal and Cu_2O crystal of material samples, respectively [5,9,11]. Here it could be seen that, although the average crystal size of the samples was not much different (the largest acheved was 22.50 nm of ZC_{250} sample, the smallest acheved was (20.08-20.36) nm of ZC_{120} and ZC_{200} samples) but it was much smaller than this data of single-phase Cu_2O sample (27.8 nm) and single-phase ZnO sample (64.5 nm) (in our previous studies) [20,21]. This is desirable for ZC NCs that have significantly reduced the average crystal size compared with their undoped single-phase materials Cu_2O or ZnO.

3.2 Scanning electron microscopy results (SEM)

The scanning electron microscopy results (SEM) of ZC_{120}, ZC_{200} and ZC_{250} nanocomposites were shown in Fig. 2. The SEM images of the ZC_{120}, ZC_{200} and ZC_{250} samples (Fig. 2) showed that the small crystals were aggregated into larger crystals in two shapes: the coral bulk shape (assigned to the aggregate shape of the ZnO crystals) intertwined with the quasi-spherical bulk shape (assigned to the aggregate shape of the Cu_2O crystals) [2,3,5]. The bulk shape of these crystals gradually grew in the material samples when hydrothermal temperature increased from (120-250) ℃.

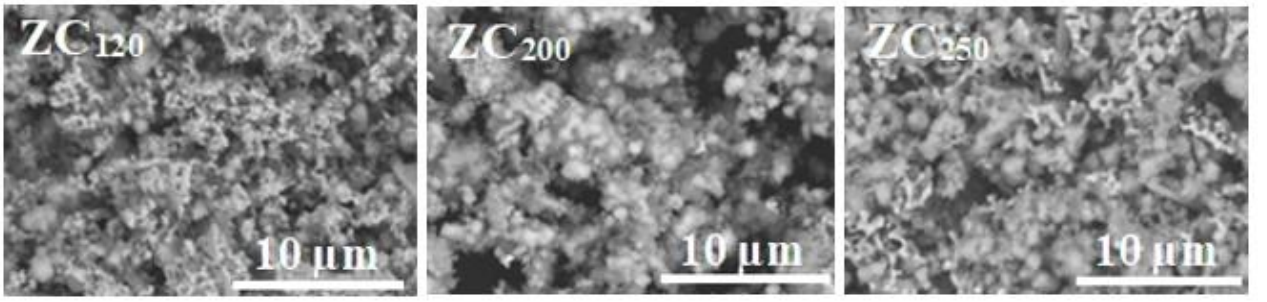

Fig. 2 Scanning electron microscopy (SEM) of the ZC_{120}, ZC_{200} and ZC_{250} samples

+ Fig. 3 was the results of the energy dispersive X-ray spectra (EDX) of ZC_{120}, ZC_{200} and ZC_{250} samples. The EDX spectra (Fig. 3) of the material samples showed that there were peaks of Cu, Zn and O elements. The higher the hydrothermal temperature of the samples (from the hydrothermal temperature of (120-250) °C), the stronger the peak intensity of Zn element was. The composition and elemental content of the ZC_{120}, ZC_{200} and ZC_{250} samples showed that: The elements ratio of Zn:Cu in the ZC_{120}, ZC_{200} and ZC_{250} samples was 0.07, 0.09 and 0.093, respectively.

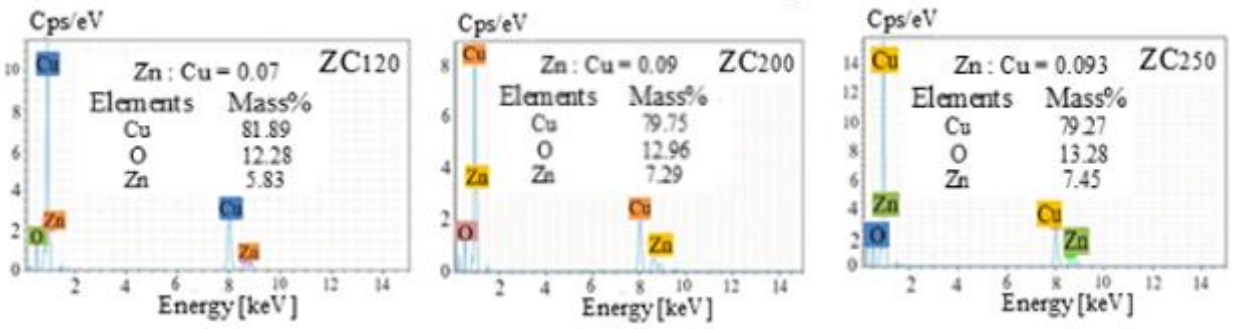

Fig. 3 Energy dispersive X-ray spectra (EDX) of ZC_{120}, ZC_{200} and ZC_{250} samples

Therefore, the molar ratios of ZnO:Cu_2O in the ZC_{120}, ZC_{200} and ZC_{250} samples were 14 %, 18 % and 18.6 %, respectively. This showed that the number of moles of ZnO in the ZC_{120}, ZC_{200} and ZC_{250} samples were lost, but not significantly compared to the number of moles of ZnO which were introduced into the original mixed solution and this was in agreement with references [2-5]. Moreover, at the high hydrothermal temperature of (200-250) °C, the number of moles of ZnO which were hybridized into the Cu_2O achieved more effective (18-18.6) % than at the low hydrothermal temperature of 120 °C (14 %).

3.3 UV-Vis absorption spectra results

The UV-Vis absorption spectra results of ZC_{120}, ZC_{200} and ZC_{250} samples were shown in Fig. 4a. The Tauc plot of $(\alpha h\nu)^{1/2}$ vs. absorbed light energy ($h\nu$) [2,9,10] of the ZC_{120}, ZC_{200}, ZC_{250} samples were shown in Fig. 4b, Fig. 4c and Fig. 4d, respectively. On the UV-Vis absorption spectra of the ZC_{120}, ZC_{200}, ZC_{250} samples (Fig. 4a), it was shown that the samples had two levels of absorption band extension: one was extended in the region wavelength of ~ 400 nm (extension of this absorption edge corresponds to the ZnO material [5-7]), after that the absorbance gradually decreased. Another level was that the absorption edge was extended in the wavelength region of $\lambda \approx$ (550-600) nm (extension of this absorption edge corresponds to the Cu_2O material [5,8-11]), after that the absorbance gradually decreased even lower. Thus, the results of UV-Vis absorption spectra showed that there was a widening of absorption edge of two material types as ZnO and Cu_2O. The corresponding Tauc plot calculated as $(\alpha h\nu)^{1/2}$ vs. $h\nu$ to determine the optical bandgap of the ZC_{120}, ZC_{200}, ZC_{250} nanocomposite samples (Fig. 4b, Fig. 4c, and Fig. 4d), the optical bandgap energy (Eg) of the ZC_{120}, ZC_{200}, ZC_{250} samples were determined as Eg ≈ 2.51 eV, 2.52 eV and 2.56 eV, respectively. This Eg value reduced more than that of ZnO single-phase material (Eg ≈ 3.37

eV [6,7]) and larger than that of Cu_2O single-phase material (Eg ≈ 2.17 eV [10-11]). This Eg value showed that it was intermediate between the Eg value of ZnO and Cu_2O materials. This showed that there was a mutual interaction between the two crystalline phases of ZnO and Cu_2O, leading to a positive change the Eg value of the fabricated nanocomposites (that was, these Eg ≈ (2.51-2.56) eV values were all in the excitation region of visible light). These determined Eg values found that there were not much difference at the hydrothermal temperatures of (120-250) ºC. But there were a good agreement with the solid UV-vis spectra results in Fig. 4a. When the hydrothermal temperature increased, the width of the absorption edge decreased (which mean that the absorbance shift gradually towards shorter wavelength) and the band gap energy increased. This was one of the desired properties for nanocomposite materials in the research works on these materials. In order to improve the application properties of the material in the visible light excitation region, as well as to enhance the activity of nanocomposites compared to the original single-phase materials [2,3,5].

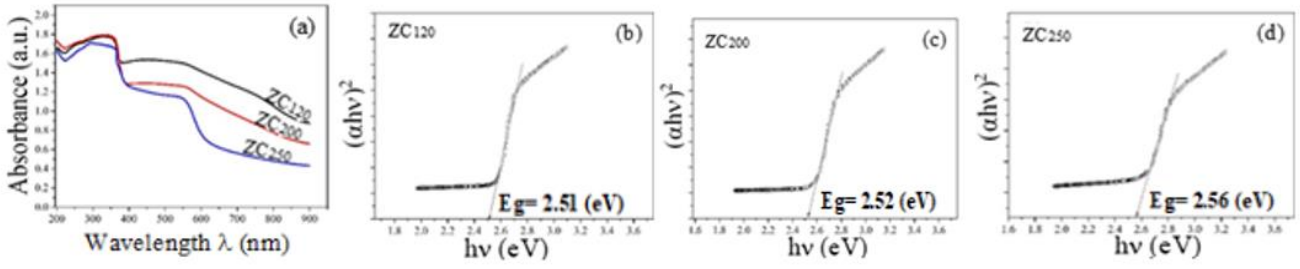

Fig. 4 a- UV-vis absorption spectra of ZC_{120}, ZC_{200} and ZC_{250} samples; b- Tauc plot of $(\alpha h\nu)^{1/2}$ vs. hν of ZC_{120} sample; c- Tauc plot of $(\alpha h\nu)^{1/2}$ vs. hν of ZC_{200} sample; d- Tauc plot of $(\alpha h\nu)^{1/2}$ vs. hν of ZC_{250} sample

4 Conclusion

The 20 % ZnO-Cu_2O nanocomposite materials (ZC NCs) have been successfully fabricated by hydrothermal method. The structural properties and characteristics of the materials had been investigated at hydrothermal temperatures of (120, 200 and 250) ℃. The samples consisted of two crystalline phases of ZnO wurtzite and Cu_2O octahedra with the calculated lattice parameters were suitable for each corresponding crystal type present in the material. The average crystal sizes of the ZC_{120}, ZC_{200} and ZC_{250} samples increased when hydrothermal temperature increased and the obtained values were 20.08 nm, 20.36 nm and 22.50 nm, respectively. EDX results showed that the percentage of moles of ZnO doped into Cu_2O has been lost but not much compared to that of the original mixed solution of 20 %, and the percentage of moles of ZnO doped into Cu_2O increased when the hydrothermal temperature increased (specifically, the percentage of moles of ZnO doped into Cu_2O was ~ 14 % at 120 ℃ and this ratio increased to (18-18.6) % at (200-250) ℃. The optical bandgap energy (Eg) of ZC NCs samples was intermediate between the Eg value of ZnO and Cu_2O materials. This Eg was reduced more than the wide bandgap energy of ZnO (~ 3.37 eV), but was larger than the band gap energy of Cu_2O (~ 2.17 eV). Specifically, the Eg bandgap energy values of the ZC_{120}, ZC_{200} and ZC_{250} samples were (2.51, 2.52 and 2.56) eV, respectively which these Eg values were all in the excitation region of visible light.

Acknowledgement

This work was funded by Hanoi University of Science and Technology (HUST) under project number AGF.2022-04. And authors also thank for the support by Hanoi University of Science and Technology (HUST) under project number CT2022.04.BKA. 05, Science and Technology Project of the Ministry of Education and Training of Vietnam.

References

1. L.Liu, W.Yang, W.Sun, Q.Li, J.K.Shang. (2014). Creation of Cu2O@TiO_2 Composite Photocatalysts with p-n Heterojunctions Formed on Exposed Cu_2O Facets, Their Energy Band Alignment Study, and Their Enhanced Photocatalytic Activity under Visible Light Illumination. *ACS Applied Materials & Interfaces*. pp.1-35.
2. O.I.Gyrdasova, E.V.Shalaeva, V.N.Krasil'nikov, L.Y.Buldakova, I.V.Baklanova, M.A. Melkozerova, M.V.Kuznetsov, M.Y.Yanchenko. (2021). Effect of Cu^+ ions on the structure, morphology, optical and photocatalytic properties of nanostructured ZnO. *Materials Characterization.* 179, 111384(1-12).
3. A.Abdolhoseinzadeh, S.Sheibani. (2019). Enhanced photocatalytic performance of Cu_2O nano-photocatalyst powder modified by ball milling and ZnO. *Advanced Powder Technology*. pp.1-11.
4. M.I.Rahmah et al. (2020). Synthesis and study photocatalytic activity of Fe_2O_3-doped ZnO nanostructure under visible light irradiation. *International Journal of Environmental Analytical Chemistry*, pp.1-14.
5. Ellen Caroline Jacobsen. (2015). Analysis of the ZnO/Cu_2O Thin Film Heterojunction for Intermediate Band Solar Cell Applications. *Norwegian University of Science and Technology*. pp.1-97.
6. E.G.Goh, X.Xu, P.G.McCormick. (2014). Effect of particle size on the UV absorbance of zinc oxide nanoparticles. *Scripta Materialia* 78-79, pp.49-52.
7. A.K.Zak, R.Razali, W.H.A.Majid, M.Darroudi. (2011). Synthesis and characterization of a narrow size distribution of zinc oxide nanoparticles. *International Journal of Nanomedicine*. 6, pp.1399-1403.
8. S.S.Sawant, A.D.Bhagwat, C.M.Mahajan. (2016). Synthesis of Cuprous Oxide (Cu2O) Nanoparticles – a Review. *Journal Nano- and Electronic Physic*s. Vol. 8 No 1, 01035(5pp).
9. M.M.Elmahdy, A.E.Shaer. (2019). Structural, optical and dielectric investigations of electrodeposited p type Cu_2O. *Journal Mater. Sci.: Materials in Electronics*. pp.1-12.
10. Y.Luo et al. (2007). Facile Synthesis of Flowerlike Cu_2O Nanoarchitectures by a Solution Phase Route. *Crystal Growth & Design.* 7(1), pp.87-92.
11. M.A. Khan et al. (2015). Surfactant Assisted Synthesis of Cuprous Oxide (Cu_2O) Nanoparticles via Solvothermal Process. *Nanoscience and Nanotechnology Research*. Vol. 3, No. 1, pp.16-22.
12. T.K.S. Wong, S. Zhuk, S. Masudy-Panah, G.K. Dalapati. (2016). Current Status and Future Prospects of Copper Oxide Heterojunction Solar Cells. *Mater. (Basel).* 9, p.271.
13. X. Zhang, Y. Xie, F. Xu, X. Liu, D. Xu. (2003). Shape-controlled synthesis of submicro-sized cuprous oxide octahedra. Inorganic Chem. *Commun.* 6(11), pp.1390-1392.
14. Y. Yu, F.P. Du, J.C. Yu, Y.Y. Zhuang, P.K. Wong. (2004). One-dimensional shape-controlled preparation of porous Cu_2O nano-whiskers by using CTAB as a template. *Journal of Solid State Chem.* 177(12), pp.4640-4647.
15. H.S. Shin, J.Y. Song, J. Yu. (2009). Template-assisted electrochemical synthesis of cuprous oxide nanowires. *Mater. Letters.* 63, pp.397-399.
16. H. Xu, W. Wang, W. Zhu. (2006). Shape evolution and size-controllable synthesis of Cu_2O octahedra and their morphology-dependent photocatalytic properties. *Journal Phys. Chem. B* 110, pp.13829-13834.
17. X. Wu. (2017). Engineering crystal orientation of p-Cu_2O on heterojunction solar cells. *Surf. Eng.* 33, pp.542.
18. S.Noda, H.Shima, H.Akinaga. (2013). Cu_2O/ZnO Heterojunction Solar Cells Fabricated by Magnetron-Sputter Deposition Method Films Using Sintered Ceramics Targets. *Journal Phys. Conf. Ser.* 433, p.012027.
19. M.Y. Shen, T. Yokouchi, S. Koyama, T. Goto. (1997). Dynamics associated with Bose-Einstein statistics of orthoexcitons generated by resonant excitations in cuprous oxide. *Phys. Review B.* 56, pp.13066-13072.
20. N.T.L.Giang, N.C. Tu, P.V. Thang, N.T.T. Mai, N.T. Lan, H.D. Chinh, T.N. Dung et al. (2021). Green synthesis of cuprous oxide (Cu_2O) nano particles using aloe vera plant. *Vietnam Catal. Adsorp.* 10(2), pp.54-58.
21. N.T.T. Mai, D.T.M. Hue, T.T.T. Huyen, N.T. Lan, N.K. Nga, T.X. Anh, T.N. Dung, H.D. Chinh, N.C. Tu, L.T.L. Anh. (2021). Effect of hexamethylene tetramine (HMTA) surfactant on the structural characteristics and photocatalytic activity of Cu-ZnO nanoparticle materials fabricated by the hydrothermal method. *Vietnam J. Catal. Adsorp*. 10(3), pp.34-39.

Khảo sát ảnh hưởng của nhiệt độ thủy nhiệt đến cấu trúc và đặc tính của nanocomposit 20 % ZnO-Cu_2O

Nguyễn Thị Tuyết Mai, Nguyễn Thị Lan, Nguyễn Kim Ngà, Tạ Ngọc Dũng, Huỳnh Đăng Chính

Viện Kĩ thuật Hóa học, Đại học Bách Khoa Hà Nội, Hà Nội, Việt Nam
mai.nguyenthituyet@hust.edu.vn

Tóm tắt: ZnO với 20 % mol được lai ghép với Cu_2O để tạo nanocomposit (20 % ZnO-Cu_2O (ZC NCs)) chế tạo theo phương pháp thủy nhiệt ở các nhiệt độ khảo sát (120, 200 và 250) °C. Các tính chất cấu trúc và đặc tính của vật liệu được nghiên cứu bởi các phép đo vật lý bao gồm: XRD, SEM, EDX và phổ UV-Vis mẫu rắn. Các kết quả cho thấy các mẫu vật liệu gồm hai pha tinh thể (ZnO wurtzit và Cu_2O octahedra) với các thông số ô mạng đã tính toán được phù hợp với mỗi loại tinh thể tương ứng của vật liệu. Kích thước tinh thể trung bình của các mẫu ZC_{120}, ZC_{200} và ZC_{250} tương ứng lần lượt là (20,08, 20,36 và 22,50) nm. Các tinh thể của các mẫu này phát triển lớn hơn khi nhiệt độ thủy nhiệt tăng. Năng lượng khe trống quang (Eg) của các mẫu ZC_{120}, ZC_{200} và ZC_{250} tương ứng lần lượt là (2,51, 2,52 và 2,56) eV. Các giá trị Eg này của các mẫu ZC NCs là trung gian giữa hai loại vật liệu ZnO (Eg ~ 3,37 eV) và Cu_2O (Eg ~ 2,17 eV) và đạt được giá trị nằm trong vùng kích thích của ánh sáng khả kiến.

Từ khóa Đồng(I) oxit, nanocomposit ZnO-Cu_2O, hạt nano Cu_2O pha tạp ZnO, bức xạ ánh sáng nhìn thấy